

A many-body marker for three-dimensional topological insulators with inversion symmetry

Federico Becca¹ and Alberto Parola²

¹*Dipartimento di Fisica, Università di Trieste, Strada Costiera 11, I-34151 Trieste, Italy*

²*Dipartimento di Scienza e Alta Tecnologia, Università dell'Insubria, Via Valleggio 11, I-22100 Como, Italy*

(Dated: May 27, 2025)

We introduce a generalization of the previously defined many-body marker for two-dimensional \mathbb{Z}_2 topological insulators [I. Gilardoni *et al.*, Phys. Rev. B **106**, L161106 (2022)] to distinguish trivial, weak-, and strong-topological insulators in three dimensions, in presence of the inversion symmetry. The marker is written in term of ground-state expectation values of position operators and can be employed to detect topological phases of interacting systems beyond mean-field approximations, e.g., within quantum Monte Carlo techniques. Here, we show that the correct results of the non-interacting limit is reproduced by the many-body marker.

I. INTRODUCTION

The groundbreaking proposals [1, 2] that established the existence of topological insulators in two spatial dimensions (resulting from spin-orbit coupling and time-reversal invariance) and their subsequent experimental confirmation [3] ignited a tremendous amount of activity in this area [4]. A remarkable achievement was the generalization to three-dimensional systems [5–7]. Classifications of insulators have been developed within the non-interacting framework [8], emphasizing the role of specific symmetries in defining distinct topological states. In particular, when only time-reversal and charge conjugation symmetries are allowed, ten classes were identified and, in each spatial dimension, five of them are topological, while the remaining ones are trivial. In general, the fingerprint of topological states is the existence of gapless excitations at the boundaries, typically referred to as edge states. In addition, the bulk of the system can be characterized by topological invariants (or markers) that, in the simplest case are given by Chern or Chern-Simons forms (in even or odd dimensions, respectively). In two dimensions, the most celebrated example is given by integer quantum Hall states, which can be stabilized even in the absence of specific symmetries. In this context, the Chern number is related to the (quantized) transverse conductivity [9]. Consequently, an infinite number of topologically different states can exist, stemming from the fact that the Chern number can assume any integer value \mathbb{Z} . Much of our understanding in this field has been obtained from studying systems within the band theory paradigm. Here, the Chern number can be computed by integrating the Berry curvature over the first Brillouin zone [9, 10]. The situation is radically different in three dimensions, where quantum Hall states do not exist. The presence of time-reversal symmetry alone fundamentally changes the situation limiting the possible states to just two classes (trivial and topological) in both two and three dimensions, leading to a \mathbb{Z}_2 invariant [8]. Nevertheless, the actual computation of topological markers is more involved than that of Chern numbers and different approaches have been suggested [11]. The

presence of additional (lattice) symmetries greatly simplify the situation, as emphasized for the case in which the inversion symmetry is present [12]. Then, the classification does not change in two dimensions, still giving rise to a single \mathbb{Z}_2 invariant. Instead, in three dimensions, four \mathbb{Z}_2 invariants emerge, distinguishing the trivial insulator from the so-called weak- and strong-topological insulators [5–7]. All these invariants can be constructed from the parity eigenvalues of the occupied orbitals at time-reversal momenta in the Brillouin zone [12].

The most significant limitation of previous attempts to define topological markers is their reliance on non-interacting systems, where a single-particle picture is used. The inherent presence of interactions in all states of matter, including band insulators, necessitates a general definition of topological insulators that accounts for electron-electron interactions. The importance of this requirement is highlighted by the one-dimensional example, which demonstrates that a non-interacting topological state may be unstable against interactions [13]. Interestingly, a generalization of the results obtained in Ref. [9] to include many-body effects has been proposed for (two-dimensional) quantum Hall states [14]. However, this approach necessitates the computation of the ground-state wave function with different (twisted) boundary conditions, posing challenges for numerical implementations [15]. Building upon Volovik's initial observation [16, 17], it has been proposed that topological aspects can be identified within the (interacting) single-particle Green's function $G(\mathbf{k}, \omega)$ [18, 19], where edge poles might become zeros without the single-particle gap closing. This possibility has been explored in order to give a topological characterization of the Mott phase of lattice models [20]. Furthermore, it has been argued that an effective Hamiltonian can be defined from $G(\mathbf{k}, 0)$, allowing the formulation of topological invariants for interacting systems [21]. A few works applied these ideas to the Bernevig-Hughes-Zhang (BHZ) [22, 23] and Hofstadter models [24] in the presence of electron-electron repulsion. Still, this kind of approaches is not always achievable, since the Green's function is not easily assessed in several numerical methods (e.g., quantum

Monte Carlo).

Within a different perspective, starting from the position operator that has been introduced within the modern theory of polarization [25], we have shown that it is possible to define a \mathbb{Z}_2 many-body marker, whose sign discriminates between trivial and topological insulators, for both one and two spatial dimensions [26]. Here, the marker is expressed as a ground-state expectation value of a suitably defined many-body operator, allowing for straightforward evaluation within various variational approaches. A first accomplishment of this strategy has been obtained within the one-dimensional BHZ model with intra-orbital Hubbard interaction [27], where the stability of trivial and topological phases have been accurately determined by using Jastrow-Slater wave functions and density-matrix renormalization group techniques [28].

Here, we further elaborate along the same direction and show that our many-body marker can be also used in three dimensions with inversion symmetry, to distinguish among trivial, weak-, and strong-topological insulators. The picture becomes particularly transparent within the non-interacting limit for models with conserved z -component of the spin (i.e., whenever the Hamiltonian commutes with S^z). In this case, the sign of our many-body marker is fully determined by the signs of the Chern numbers within two planes in the Brillouin zone. This outcome reminds the fact that the integral of the (three-dimensional) Chern-Simons form equals the parity of the sum of the Chern numbers computed at two fixed planes in the k -space (e.g., $k_z = 0$ and π on the cubic lattice) [29]. In addition, the marker is also simply related to the parity eigenvalues of the occupied orbitals at time-reversal invariant momenta (TRIM). A similar structure is also obtained, within the non-interacting limit, for general models that do not commute with S^z . Our topological marker allows one to consider interacting models by using variational or projection quantum Monte Carlo techniques. These studies require heavy numerical calculations and, therefore, are left for future investigations.

The paper is organized as follows: in section II we give the general definitions for the lattice structure and the properties of the Hamiltonian; in section III, we define the topological marker, discussing its expression in the non-interacting limit; in section IV, we report the calculations for two specific models that have been introduced in the past; finally, in section V, we draw our conclusions.

II. GENERAL ASPECTS

A d -dimensional Bravais lattice is defined by a set of d primitive vectors \mathbf{a}_i , such that $\mathbf{R} = \sum_j l_j \mathbf{a}_j$, where l_j are integers. The vectors in the reciprocal space are defined by the usual condition $\mathbf{a}_i \cdot \mathbf{b}_j = 2\pi\delta_{ij}$; the reciprocal-lattice vectors are then given by $\mathbf{G} = \sum_j m_j \mathbf{b}_j$, where m_j are integers. The geometry of a finite cluster with periodic boundary conditions is identified by d trans-

lation vectors $\mathbf{T}_i = \sum_j N_{ij} \mathbf{a}_j$ (where N_{ij} is a matrix of integers) and the quantization rule in the Brillouin zone is simply $x_i = \mathbf{q} \cdot \mathbf{a}_i = 2\pi \sum_j (N^{-1})_{ij} n_j$ (where n_i are integers). In this work, we focus our attention on $d = 3$ and take clusters defined by a diagonal matrix with $N_{11} = L_1$, $N_{22} = L_2$, and $N_{33} = L_3$. The total number of unit cells is $N = L_1 \times L_2 \times L_3$. In this case, we have that $x_i = 2\pi n_i / L_i$, with $n_i = 0, \dots, L_i - 1$ for $i = 1, 2, 3$. Setting $\mathbf{q} = \sum_i q_i \mathbf{b}_i$, the quantization simply gives $q_i = n_i / L_i$.

Let us consider a generic non-interacting and translationally invariant model, with N_o orbitals per primitive cell, in a cluster with N_c cells and periodic-boundary conditions. Then, the Hamiltonian can be written in Fourier space in terms of a k -dependent $2N_o \times 2N_o$ matrix $h(\mathbf{k})$ (that includes both orbital and spin degrees of freedom):

$$\hat{\mathcal{H}} = \sum_{\mathbf{k}} \sum_{\eta, \sigma, \eta', \sigma'} h_{\eta, \eta'}^{\sigma, \sigma'}(\mathbf{k}) \hat{c}_{\mathbf{k}, \eta, \sigma}^\dagger \hat{c}_{\mathbf{k}, \eta', \sigma'}, \quad (1)$$

where $\hat{c}_{\mathbf{k}, \eta, \sigma}^\dagger$ ($\hat{c}_{\mathbf{k}, \eta, \sigma}$) is the fermionic creator (annihilator) operator of an electron of momentum \mathbf{k} , orbital η and spin σ . On any Bravais lattice, these fermionic operators are the Fourier transformed of $\hat{c}_{\mathbf{R}, \eta, \sigma}^\dagger$ and $\hat{c}_{\mathbf{R}, \eta, \sigma}$, which create and destroy an electron on the site \mathbf{R} , orbital η , and spin σ .

The Hamiltonian (1) can be easily diagonalized by a canonical transformation:

$$\hat{\phi}_{\mathbf{k}, a}^\dagger = \sum_{\eta, \sigma} u_{\mathbf{k}, a}(\eta, \sigma) \hat{c}_{\mathbf{k}, \eta, \sigma}^\dagger, \quad (2)$$

where $a = 1, \dots, 2N_o$ indicates the band index and $u_{\mathbf{k}, a}(\eta, \sigma)$ are eigenvectors of the matrix $h_{\eta, \eta'}^{\sigma, \sigma'}(\mathbf{k})$. Then, the Bloch functions are defined by

$$\psi_{\mathbf{k}, a}(\mathbf{R}, \eta, \sigma) = \langle 0 | \hat{c}_{\mathbf{R}, \eta, \sigma} \hat{\phi}_{\mathbf{k}, a}^\dagger | 0 \rangle = \frac{e^{i\mathbf{k} \cdot \mathbf{R}}}{\sqrt{N_c}} u_{\mathbf{k}, a}(\eta, \sigma). \quad (3)$$

It is convenient to express the $2N_o \times 2N_o$ matrix $h(\mathbf{k})$ in terms of a tensor product of 2×2 Pauli matrices σ_α (with $\alpha = 0, \dots, 3$, including $\sigma_0 = \mathbb{1}$) and $N_o \times N_o$ matrices (that, in the simplest case with $N_o = 2$ are also Pauli matrices τ_β), which act on the spin and orbital indices, respectively. Here, we focus on the cases in which the Hamiltonian $\hat{\mathcal{H}}$ is invariant under inversion and time-reversal symmetries. The (unitary) inversion operator $\hat{\mathcal{P}}$ transforms the fermionic operator as

$$\hat{\mathcal{P}}^{-1} \hat{c}_{\mathbf{R}, \eta, \sigma} \hat{\mathcal{P}} = \sum_{\eta'} V_{\eta, \eta'} \hat{c}_{-\mathbf{R}, \eta', \sigma}, \quad (4)$$

where V is a $N_o \times N_o$ (model-dependent) unitary matrix acting on band indices. Instead, the (anti-unitary) time-reversal operator $\hat{\mathcal{T}}$ gives

$$\hat{\mathcal{T}}^{-1} \hat{c}_{\mathbf{R}, \eta, \uparrow} \hat{\mathcal{T}} = \hat{c}_{\mathbf{R}, \eta, \downarrow}, \quad (5)$$

$$\hat{\mathcal{T}}^{-1} \hat{c}_{\mathbf{R}, \eta, \downarrow} \hat{\mathcal{T}} = -\hat{c}_{\mathbf{R}, \eta, \uparrow}, \quad (6)$$

and includes complex conjugation, i.e., $\hat{\mathcal{T}}^{-1}z\hat{\mathcal{T}} = z^*$ for any complex number z . Then, it is possible to define the corresponding $2N_o \times 2N_o$ matrices that act on the matrix $h(\mathbf{k})$. The inversion $P = \mathbb{1} \otimes V$ is a symmetry of the model provided $P^{-1}h(\mathbf{k})P = h(-\mathbf{k})$, while the time-reversal $T = i\sigma_y \otimes \mathbb{1}K$ (where K takes the complex conjugation) requires $T^{-1}h(\mathbf{k})T = h^*(-\mathbf{k})$. The first property implies that it is always possible to choose the eigenstates of $h(\mathbf{k})$ in such a way that $u_{-\mathbf{k},a}(\eta, \sigma) = P^\dagger u_{\mathbf{k},a}(\eta, \sigma)$ (provided $-\mathbf{k} \neq \mathbf{k} + \mathbf{G}$), while for $-\mathbf{k} = \mathbf{k} + \mathbf{G}$, the parity operator P commutes with $h(\mathbf{k})$ and then it is possible to choose $u_{\mathbf{k},a}(\eta, \sigma)$ as an eigenstate of P with eigenvalue $\xi_a(\mathbf{k}) = \pm 1$. Instead, time-reversal symmetry leads to Kramers degeneracy.

III. THE \mathbb{Z}_2 MANY-BODY MARKER

The central object of our analysis is the real space, spin-projected operator, previously introduced to distinguish between metals and insulators [25]:

$$\hat{Z}_\sigma(\delta\mathbf{k}) = e^{i\delta\mathbf{k} \cdot \sum_{\mathbf{R}} \mathbf{R} \hat{n}_{\mathbf{R},\sigma}}, \quad (7)$$

where \mathbf{R} runs over the lattice vectors of the cluster, $\delta\mathbf{k}$ is a momentum shift, quantized according to the geometry of the cluster (see below), and $\hat{n}_{\mathbf{R},\sigma} = \sum_{\eta} \hat{c}_{\mathbf{R},\eta,\sigma}^\dagger \hat{c}_{\mathbf{R},\eta,\sigma}$ is the number operator of electrons on site \mathbf{R} with spin σ (summed over the orbital index η).

Under parity transformation, we have that $\hat{P}^{-1} \hat{n}_{\mathbf{R},\sigma} \hat{P} = \hat{n}_{-\mathbf{R},\sigma}$ leading to:

$$\hat{P}^{-1} \hat{Z}_\sigma(\delta\mathbf{k}) \hat{P} = e^{-i\delta\mathbf{k} \cdot \sum_{\mathbf{R}} \mathbf{R} \hat{n}_{\mathbf{R},\sigma}} = \hat{Z}_\sigma^\dagger(\delta\mathbf{k}). \quad (8)$$

Therefore, whenever the parity is not broken, the ground-state average $\langle \Psi | \hat{Z}_\sigma(\delta\mathbf{k}) | \Psi \rangle$ is always real, i.e., its phase can be either 0 or π (modulo 2π).

In Ref. [26], we studied two-dimensional lattice models with $N_o = 2$, showing that the \mathbb{Z}_2 topological character is uniquely identified by the (quantized) phase of the marker:

$$\rho_\sigma = \frac{\langle \Psi | \hat{Z}_\sigma(\delta\mathbf{k}_1 + \delta\mathbf{k}_2) | \Psi \rangle}{\langle \Psi | \hat{Z}_\sigma(\delta\mathbf{k}_1) | \Psi \rangle \langle \Psi | \hat{Z}_\sigma(\delta\mathbf{k}_2) | \Psi \rangle}, \quad (9)$$

where the two elementary momenta are taken as $\delta\mathbf{k}_n = \mathbf{b}_n/L_n$. For non-interacting models that commute with S^z , this marker is simply related to the Chern number of the occupied band. Remarkably, even though the marker ρ_σ is defined for a given spin projection, its validity is not limited to models where the total spin along z is conserved. In fact, we showed that even including a spin-orbit interaction (e.g., the Rashba term in the Kane-Mele model) the definition of Eq. (9) allows one to discriminate between trivial and topological phases [26]. In the following, we show that the same marker gives a way to distinguish among trivial, weak-, and strong-topological insulators in three dimensions.

A. The non-interacting limit: models with conserved S^z

Here, we focus on models where the total spin along z commutes with the Hamiltonian (1). In this case, the single-particle spectrum consists of N_o bands per spin projection. In the following, we perform the calculation for the lowest-energy m bands, assuming that a gap separates them from the other ones. This circumstance corresponds to an electron density per spin projection $\nu = m/N_o$. The many-body ground state $|\Psi\rangle$ is the Slater determinant of the single particle orbitals of the occupied bands, which, in this case, is factorized into spin up and down components. The $\hat{Z}_\sigma(\delta\mathbf{k})$ operator acts only on the states of the lowest (occupied) spin- σ bands, defining the $mN_c \times mN_c$ overlap matrix:

$$O_{(\mathbf{q},a),(\mathbf{p},b)} = \langle \psi_{\mathbf{q},a} | \hat{Z}_\sigma(\delta\mathbf{k}) | \psi_{\mathbf{p},b} \rangle = \delta_{\mathbf{q},\mathbf{p}+\delta\mathbf{k}} A_{a,b}^\sigma(\mathbf{q}), \quad (10)$$

where the $m \times m$ matrices $A^\sigma(\mathbf{q})$ are defined by:

$$A_{a,b}^\sigma(\mathbf{q}) = \sum_{\eta} u_{\mathbf{q},a}^*(\eta, \sigma) u_{\mathbf{q}-\delta\mathbf{k},b}(\eta, \sigma). \quad (11)$$

The elementary properties of Slater determinants imply that:

$$\langle \Psi | \hat{Z}_\sigma(\delta\mathbf{k}) | \Psi \rangle = \det\{O_{(\mathbf{q},a),(\mathbf{p},b)}\}. \quad (12)$$

Given the specific form of the overlap matrix, for an even number of sites in the cluster N_c , we have:

$$\langle \Psi | \hat{Z}_\sigma(\delta\mathbf{k}) | \Psi \rangle = \prod_{\mathbf{q}} \det\{A_{a,b}^\sigma(\mathbf{q})\}. \quad (13)$$

Inversion symmetry allows us to further simplify this expression. We already pointed out that whenever $-\mathbf{q} \neq \mathbf{q} + \mathbf{G}$ it is always possible to choose $u_{-\mathbf{q},a}(\eta, \sigma) = P^\dagger u_{\mathbf{q},a}(\eta, \sigma)$, while for $-\mathbf{q} = \mathbf{q} + \mathbf{G}$, $u_{\mathbf{q},a}(\eta, \sigma)$ is an eigenstate of P with eigenvalue $\xi_a(\mathbf{q}) = \pm 1$. Then, it follows that the overlap matrix $A_{a,b}^\sigma(\mathbf{q})$ satisfies a simple transformation property when both \mathbf{q} and $\mathbf{q} + \delta\mathbf{k}$ are not invariant under inversion (modulo a reciprocal lattice vector):

$$\begin{aligned} A_{b,a}^\sigma(-\mathbf{q}) &= \sum_{\eta} u_{-\mathbf{q},b}^*(\eta, \sigma) u_{-\mathbf{q}-\delta\mathbf{k},a}(\eta, \sigma) \\ &= \sum_{\eta} [P^\dagger u_{\mathbf{q},b}(\eta, \sigma)]^* P^\dagger u_{\mathbf{q}+\delta\mathbf{k},a}(\eta, \sigma) \\ &= \sum_{\eta} u_{\mathbf{q},b}^*(\eta, \sigma) u_{\mathbf{q}+\delta\mathbf{k},a}(\eta, \sigma) \\ &= [A_{a,b}^\sigma(\mathbf{q} + \delta\mathbf{k})]^*. \end{aligned} \quad (14)$$

Instead, if \mathbf{q} remains unchanged under inversion, the transformation property acquires an extra-factor:

$$\begin{aligned}
A_{b,a}^\sigma(-\mathbf{q}) &= \sum_{\eta} u_{-\mathbf{q},b}^*(\eta, \sigma) u_{-\mathbf{q}-\delta\mathbf{k},a}(\eta, \sigma) \\
&= \sum_{\eta} u_{\mathbf{q},b}^*(\eta, \sigma) P^\dagger u_{\mathbf{q}+\delta\mathbf{k},a}(\eta, \sigma) \\
&= \sum_{\eta} [P^\dagger u_{\mathbf{q},b}(\eta, \sigma)]^* u_{\mathbf{q}+\delta\mathbf{k},a}(\eta, \sigma) \\
&= \xi_b(\mathbf{q}) [A_{a,b}^\sigma(\mathbf{q} + \delta\mathbf{k})]^*. \tag{15}
\end{aligned}$$

Setting $\delta\mathbf{k}_n = \mathbf{b}_n/L_n$, in a cluster with an even number of sites L_n , the factors $\det\{A_{a,b}^\sigma(-\mathbf{q})\}$ and $\det\{A_{a,b}^\sigma(\mathbf{q} + \delta\mathbf{k}_n)\}$ always come in pairs. As a consequence, the sign of the product over all wavevectors \mathbf{q} in Eq. (13) is just $\prod_i \delta_i$, with $\delta_i = \prod_a \xi_a(\mathbf{\Gamma}_i)$, where the index i runs over all the TRIM wavevectors $\mathbf{\Gamma}_i$ (that are left unchanged under inversion) and the index a runs over all the occupied bands.

In conclusion, when the number of sites of the cluster in each direction L_j is even, the sign of the ground state average of each position operator $\hat{Z}_\sigma(\delta\mathbf{k}_n)$ (with $n = 1, 2, 3$) equals the product of the eight δ_i and coincides with the \mathbb{Z}_2 invariant that identifies the strong-topological phase. In addition, the three other (weak) \mathbb{Z}_2 topological invariants can be evaluated by taking a cluster where one of the L_j (for $j \neq n$) is odd. In this way, four of the special points $\mathbf{\Gamma}_i$ are no longer present, due to the quantization rules, and the sign of the ground-state average of $\hat{Z}_\sigma(\delta\mathbf{k}_n)$ is just the product of the four remaining δ_i . The trivial phase occurs when all topological invariants equal +1; the weak-topological phases differ from the trivial insulator because of a negative value of at least one (in fact two) of the ground-state averages of $\hat{Z}_\sigma(\delta\mathbf{k}_n)$ in clusters where one of the L_j (with $j \neq n$) is odd; finally, the strong-topological phase appears when the ground state average of $\hat{Z}_\sigma(\delta\mathbf{k}_n)$ is negative (for any choice of n) in clusters with even number of sites L_j in all directions.

The ground-state averages of $\hat{Z}_\sigma(\delta\mathbf{k}_n)$ combine in the definition of the topological marker (9) previously introduced in two dimensional models. In the adopted definition, both $\delta\mathbf{k}_1$ and $\delta\mathbf{k}_2$ have no components along \mathbf{b}_3 , implying that all expectation values may be factorized into a product over the third component of $\mathbf{q} = \sum_i q_i \mathbf{b}_i$ of q_3 -dependent factors, which immediately leads to:

$$\rho_\sigma = \prod_{q_3} \rho_\sigma(q_3); \tag{16}$$

here, $\rho_\sigma(q_3)$ is the two-dimensional \mathbb{Z}_2 marker at fixed q_3 , i.e., the one evaluated along the $(\mathbf{b}_1, \mathbf{b}_2)$ planes of the Brillouin zone at the given q_3 . In Ref. [26], we showed that, in the thermodynamic limit ($N_c \rightarrow \infty$) and for the case of a single band, the phase of $\rho_\sigma(q_3)$ is just π times the spin Chern number of that plane. As previously shown, the sign of this product over all q_3 's is determined by the special points invariant under inversion

symmetry: $q_3 = 0$ and, when allowed by the quantization condition, $q_3 = 1/2$. Therefore, only the Chern numbers of these two planes contain the relevant information for the identification of a topological insulator.

In spatially isotropic models, the marker can be equivalently used to identify the three phases: if its sign is positive for both L_3 even and odd, the two spin Chern numbers at $q_3 = 0$ and $q_3 = 1/2$ are even and the insulator is trivial. If ρ_σ is positive for L_3 even while is negative for L_3 odd, the two spin Chern numbers at $q_3 = 0$ and $q_3 = 1/2$ are both odd and the topological insulator is weak. Finally, if ρ_σ is negative for L_3 even, the two spin Chern numbers at $q_3 = 0$ and $q_3 = 1/2$ have different signs and the topological insulator is strong.

B. The non-interacting limit: The general cases

In the previous part, we showed that the position operator contains the relevant information required to identify the topological phases in non-interacting models where S^z commutes with the Hamiltonian. In fact, in these cases, the label σ selects one state of the Kramers doublet and allows us to evaluate the \mathbb{Z}_2 invariant. However, when the total spin along z does not commute with the Hamiltonian, the $\hat{Z}_\sigma(\delta\mathbf{k})$ operator mixes the states of the Kramers doublets, spoiling the mathematical demonstration and making the connection to the eigenvalues of the parity operator $\xi_a(\mathbf{\Gamma}_i)$ less transparent. Still, we consider the spin-projected operator (e.g., with spin up) also in such a case, appealing to adiabatic continuity between the model of interest and a model where S^z is conserved, provided that the gaps at the TRIM points do not close during the switching on of the non-conserving terms. The correctness of this procedure has been already checked in two dimensions [26] in the simplest case with $N_o = 2$, and is now adopted also in three dimensions. The explicit expression for the evaluation of the ground state average of $\hat{Z}_\sigma(\delta\mathbf{k})$ is reported in Appendix A.

IV. SPECIFIC MODELS

In the following, we illustrate the results for two specific cases that have been introduced in the past, i.e., the BHZ model on the cubic lattice [30] and the Fu-Kane-Mele (FKM) model on the diamond lattice [5]. In both cases, we have that $N_o = 2$, thus simplifying the actual calculations.

A. The BHZ model on the cubic lattice

The Hamiltonian is translationally invariant but does not conserve the z component of the total spin. The non-interacting case is written in terms of a 4×4 matrix $h(\mathbf{k})$

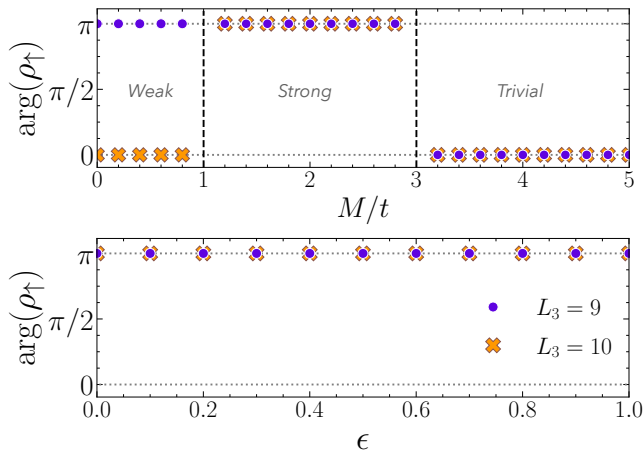


Figure 1: Upper panel: the sign of the many-body marker ρ_\uparrow of Eq. (9) for the BHZ (or equivalently the FKM), see Eq. (17) for $\lambda/t = 0.3$ and $\epsilon = 1$ as a function of M/t . The results for two clusters with $L_1 = L_2 = 10$ and $L_3 = 10$ or 9 are reported. Lower panel: the sign of ρ_\uparrow for $M/t = 2$ (within the strong-topological insulator) as a function of ϵ (here, $\epsilon = 1$ corresponds to the original model and $\epsilon = 0$ to the model that commutes with the total spin along z).

is defined by:

$$h(\mathbf{k}) = \sum_{\alpha=1}^5 d_\alpha(\mathbf{k}) \Gamma_\alpha, \quad (17)$$

where $\Gamma_1 = \sigma_z \otimes \tau_x$, $\Gamma_2 = -\mathbb{1} \otimes \tau_y$, $\Gamma_3 = \sigma_x \otimes \tau_x$, $\Gamma_4 = \sigma_y \otimes \tau_x$, and $\Gamma_5 = \mathbb{1} \otimes \tau_z$; the coefficients are given by [22]:

$$\begin{aligned} d_1(\mathbf{k}) &= \lambda \sin k_x, \\ d_2(\mathbf{k}) &= \lambda \sin k_y, \\ d_3(\mathbf{k}) &= \lambda \sin k_z, \\ d_4(\mathbf{k}) &= 0, \\ d_5(\mathbf{k}) &= M - t(\cos k_x + \cos k_y + \cos k_z). \end{aligned}$$

The model is time-reversal invariant and the inversion symmetry is given by $P = \mathbb{1} \otimes \tau_z$. In addition, the pres-

ence of the chiral symmetry $C = \sigma_y \otimes \tau_y$, which anticommutes with $h(\mathbf{k})$ and gives rise to a particle-hole symmetric spectrum, i.e., two (doubly degenerate) bands with $\epsilon(\mathbf{k}) = \pm \sqrt{\sum_\alpha d_\alpha^2(\mathbf{k})}$. At half filling, a finite gap is present, except for $M/t = \pm 1$ and $M/t = \pm 3$, where Dirac points appear at the Fermi level. Taking $M/t \geq 0$, the ground state is known to be a trivial insulator for $M/t > 3$, a strong-topological insulator for $1 < M/t < 3$, and a weak-topological insulator for $0 \leq M/t < 1$.

The Γ_3 term is responsible for the non-conservation of the z component of the spin. Then, we can generalize the model by introducing an additional parameter ϵ in front of this term, i.e., $d_3(\mathbf{k}) \rightarrow \epsilon d_3(\mathbf{k})$, and study how the marker evolves from the original model with $\epsilon = 1$ to the model that commutes with the total spin along z (with $\epsilon = 0$). Notice that for $\epsilon = 0$, the spectrum is gapless for $0 \leq M/t \leq 3$, but the Dirac points are shifted to incommensurate values for k_z . Still, the calculation of the sign of ρ_σ is not affected by this fact, since it depends only on specific planes in the Brillouin zone. We evaluate the marker ρ_\uparrow for $L_1 = L_2 = 10$ and either $L_3 = 10$ or $L_3 = 9$ (its sign depending only on the parity of L_i , in agreement with the previous analysis, with no size effects). The results are shown in Fig. 1, for $\epsilon = 1$ varying M/t and for $M/t = 2$ varying ϵ . In the former case, for $M/t > 3$, the marker is *positive* for both values of L_3 (confirming the fact that the ground state is a trivial insulator); conversely, for $1 < M/t < 3$, the marker is *negative* for $L_3 = 10$ (corresponding to a strong-topological insulator); finally, for $0 \leq M/t < 1$, ρ_\uparrow is *positive* for $L_3 = 10$ and *negative* for $L_3 = 9$ (indicating a weak-topological insulator).

B. The FKM model on the diamond lattice

The FKM model is defined on the diamond lattice (a face-centered cubic lattice with a two-site basis) and is given by the same expression of Eq. (17) with $\Gamma_1 = \mathbb{1} \otimes \tau_x$, $\Gamma_2 = \mathbb{1} \otimes \tau_y$, $\Gamma_3 = \sigma_x \otimes \tau_z$, $\Gamma_4 = \sigma_y \otimes \tau_z$, and $\Gamma_5 = \sigma_z \otimes \tau_z$. The coefficients are given by [5]

$$\begin{aligned} d_1(\mathbf{k}) &= M + t(\cos x_1 + \cos x_2 + \cos x_3), \\ d_2(\mathbf{k}) &= t(\sin x_1 + \sin x_2 + \sin x_3), \\ d_3(\mathbf{k}) &= \lambda [\sin x_2 - \sin x_3 - \sin(x_2 - x_1) + \sin(x_3 - x_1)], \\ d_4(\mathbf{k}) &= \lambda [\sin x_3 - \sin x_1 - \sin(x_3 - x_2) + \sin(x_1 - x_2)], \\ d_5(\mathbf{k}) &= \lambda [\sin x_1 - \sin x_2 - \sin(x_1 - x_3) + \sin(x_2 - x_3)], \end{aligned}$$

where $M = 1 + \delta t$ (as defined in the original work [5]) and $x_i = \mathbf{k} \cdot \mathbf{a}_i$. As in the BHZ model, the Hamil-

tonian is time-reversal invariant. In addition, the inversion symmetry is given by $P = \mathbb{1} \otimes \tau_x$. Also in

this case there are two (doubly degenerate) bands with $\epsilon(\mathbf{k}) = \pm\sqrt{\sum_{\alpha} d_{\alpha}^2(\mathbf{k})}$. Within the present choice of the “mass” term M , the FKM and BHZ models share the same ground-state phase diagram. In this case, the limit in which the Hamiltonian commutes with the total spin along z is obtained by introducing the parameter ϵ in front of both $d_3(\mathbf{k})$ and $d_4(\mathbf{k})$ terms. The results for the sign of the marker coincide with the ones reported before in the BHZ model, see Fig. 1.

V. CONCLUSIONS

In summary, we have shown that the local many-body marker of Eq. (9), which we introduced to distinguish \mathbb{Z}_2 topological insulators in two spatial dimensions [26], can be also used to discriminate among trivial, weak-, and strong-topological insulators in three dimensions, in presence of inversion symmetry. Explicit calculations in non-interacting limits have been reported. In particular, the presence of the inversion symmetry forces the marker to be real and the nature of the insulator may be extracted from its sign. Within non-interacting models in which S^z is conserved, the sign is determined by the parity eigenvalues of the occupied orbitals at time-reversal momenta in the Brillouin zone, thus reproducing the results obtained in Ref. [12]. For general models, with non conserved S^z , this correspondence is no longer transparent, but it is expected to remain whenever it is possible to adiabatically switch-off the non-conserving terms in the Hamiltonian without closing the gap at the TRIM points.

Most importantly, since our marker is not based upon the single-particle picture, it can be employed also to assess the properties of electronic models in presence of electron-electron interactions, by computing ground-state expectation values, which are accessible within quantum Monte Carlo approaches, including the variational one (as recently done for the BHZ model with Hubbard and nearest-neighbor density-density interactions [28]). Still, these kind of calculations in three dimensions require intensive numerical efforts and, therefore, are left for future studies.

Acknowledgements

We thank A. Marrazzo, L. Balents, and G. Sangiovanni for useful discussions on topological markers. We also are

indebted to R. Favata for discussions and for preparing the figure.

Appendix A: Details of the general case

Here, we report the derivation of the explicit expression of the ground-state average of $\hat{Z}_{\uparrow}(\delta\mathbf{k})$ in models where S^z is non conserved. The single-particle orbitals are defined in Eq. (3). As before, we consider a model with N_o orbitals per Bravais lattice site, implying $2N_o$ bands, $2m$ of which are occupied. In this case, the $2mN_c \times 2mN_c$ overlap matrix introduced in Eq. (10) is given by:

$$O_{(\mathbf{q},a),(\mathbf{p},b)} = \delta_{\mathbf{q},\mathbf{p}+\delta\mathbf{k}} A_{a,b}^{\uparrow}(\mathbf{q}) - \delta_{\mathbf{q},\mathbf{p}} B_{a,b}^{\downarrow}(\mathbf{q}), \quad (\text{A1})$$

where the two $2m \times 2m$ matrices $A^{\uparrow}(\mathbf{q})$ and $B^{\downarrow}(\mathbf{q})$ are defined by

$$A_{a,b}^{\uparrow}(\mathbf{q}) = \sum_{\eta} u_{\mathbf{q},a}^*(\eta, \uparrow) u_{\mathbf{q}-\delta\mathbf{k},b}(\eta, \uparrow), \quad (\text{A2})$$

$$B_{a,b}^{\downarrow}(\mathbf{q}) = - \sum_{\eta} u_{\mathbf{q},a}^*(\eta, \downarrow) u_{\mathbf{q},b}(\eta, \downarrow). \quad (\text{A3})$$

In order to evaluate the determinant of the overlap matrix, it is convenient to investigate the corresponding eigenvalue problem:

$$A^{\uparrow}(\mathbf{q}) x(\mathbf{q} - \delta\mathbf{k}) - B^{\downarrow}(\mathbf{q}) x(\mathbf{q}) = \lambda x(\mathbf{q}), \quad (\text{A4})$$

which defines the recurrence relation:

$$x(\mathbf{q} - \delta\mathbf{k}) = \left\{ \lambda [A^{\uparrow}(\mathbf{q})]^{-1} + [A^{\uparrow}(\mathbf{q})]^{-1} B^{\downarrow}(\mathbf{q}) \right\} x(\mathbf{q}). \quad (\text{A5})$$

Let us now take $\delta\mathbf{k} = \delta\mathbf{k}_n = \mathbf{b}_n/L_n$. Then, the eigenvalue problem reduces to a set of $2mL_n \times 2mL_n$ blocks, since every value of \mathbf{q} only couples to $\mathbf{q} - j\delta\mathbf{k}_n$, with $j = 0, \dots, L_n - 1$, and $L_n\delta\mathbf{k}_n$ equals \mathbf{b}_n , a vector of the reciprocal lattice. Therefore, starting from a vector \mathbf{q}_{\perp} , which has no component along \mathbf{b}_n (i.e., such that $\mathbf{q} \cdot \mathbf{a}_n = 0$) and iterating $L_n - 1$ times, we get:

$$x(\mathbf{q}_{\perp} - L_n\delta\mathbf{k}_n) = \left\{ \prod_{j=0}^{L_n-1} \left\{ \lambda [A^{\uparrow}(\mathbf{q}_{\perp} - j\delta\mathbf{k}_n)]^{-1} + [A^{\uparrow}(\mathbf{q}_{\perp} - j\delta\mathbf{k}_n)]^{-1} B^{\downarrow}(\mathbf{q}_{\perp} - j\delta\mathbf{k}_n) \right\} \right\} x(\mathbf{q}_{\perp}), \quad (\text{A6})$$

where the product is ordered in j . Since $x(\mathbf{q} - L_n \delta \mathbf{k}_n) \equiv x(\mathbf{q})$, this relation implies that the $2m \times 2m$ matrix

$$M(\mathbf{q}_\perp) = \prod_{j=0}^{L_n-1} \{ \lambda [A^\dagger(\mathbf{q}_\perp - j\delta \mathbf{k}_n)]^{-1} + [A^\dagger(\mathbf{q}_\perp - j\delta \mathbf{k}_n)]^{-1} B^\dagger(\mathbf{q}_\perp - j\delta \mathbf{k}_n) \} \quad (\text{A7})$$

has an eigenvalue equal to one. Thus, the corresponding secular equation is $\det\{M(\mathbf{q}_\perp) - \mathbb{1}\} = 0$ for each choice of \mathbf{q}_\perp . As a result, the overlap matrix is a block matrix (each block being a $2mL_n \times 2mL_n$ matrix), and its determinant is the product over \mathbf{q}_\perp of the determinants of each block. The determinant of every block can be easily computed: The secular equation is a polynomial of de-

gree $2mL_n$ in λ , e.g., $C(\lambda - \lambda_1) \dots (\lambda - \lambda_{2mL_n})$, where C is a constant and λ_i are the $2mL_n$ eigenvalues. From the factorization property, it follows that the determinant of each block matrix equals the ratio between the term of zero degree in λ and the term of degree $2mL_n$ in the secular equation:

$$R(\mathbf{q}_\perp) = \frac{\det\{\prod_{j=0}^{L_n-1} [A^\dagger(\mathbf{q}_\perp - j\delta \mathbf{k}_n)]^{-1} B^\dagger(\mathbf{q}_\perp - j\delta \mathbf{k}_n) - \mathbb{1}\}}{\det\{\prod_{j=0}^{L_n-1} [A^\dagger(\mathbf{q}_\perp - j\delta \mathbf{k}_n)]^{-1}\}}. \quad (\text{A8})$$

Finally, the determinant of the full overlap matrix is the product over \mathbf{q}_\perp of these factors:

$$\langle \Psi | \hat{Z}_\uparrow(\delta \mathbf{k}_n) | \Psi \rangle = \prod_{\mathbf{q}_\perp} R(\mathbf{q}_\perp). \quad (\text{A9})$$

Inversion symmetry allows us to further simplify this expression. Let us consider the pair of terms corresponding to \mathbf{q}_\perp and $-\mathbf{q}_\perp$ (modulo a reciprocal lattice vector) in the product of Eq. (A9), assuming that they differ from the TRIM (i.e., that $\mathbf{q}_\perp \neq \Gamma_i$). From Eq. (14), which remains valid also in non spin conserving models, it follows

that:

$$\begin{aligned} \det A^\dagger(-\mathbf{q}_\perp - j\delta \mathbf{k}_n) &= \det [A^\dagger(\mathbf{q}_\perp + (j+1)\delta \mathbf{k}_n)]^\dagger \\ &= [\det A^\dagger(\mathbf{q}_\perp - (L_n - 1 - j)\delta \mathbf{k}_n)]^*. \end{aligned} \quad (\text{A10})$$

Therefore, the product of the terms \mathbf{q}_\perp and $-\mathbf{q}_\perp$ in the denominator of Eq. (A9) always gives a positive number.

A similar argument holds also for the expression in the numerator, although the derivation is less straightforward:

$$\det \left\{ \prod_{j=0}^{L_n-1} [A^\dagger(-\mathbf{q}_\perp - j\delta \mathbf{k}_n)]^{-1} B^\dagger(-\mathbf{q}_\perp - j\delta \mathbf{k}_n) - \mathbb{1} \right\} = \left[\det \left\{ \prod_{j=0}^{L_n-1} [A^\dagger(\mathbf{q}_\perp - j\delta \mathbf{k}_n)]^{-1} B^\dagger(\mathbf{q}_\perp - j\delta \mathbf{k}_n) - \mathbb{1} \right\} \right]^*. \quad (\text{A11})$$

Therefore, the sign of $\langle \Psi | \hat{Z}_\uparrow(\delta \mathbf{k}_n) | \Psi \rangle$ in Eq. (A9) is determined by the factors corresponding to momenta \mathbf{q}_\perp equal to the TRIM Γ_i that are orthogonal to \mathbf{a}_n .

In the simplest case of two-band models, it is easy to show that the sign of $\langle \Psi | \hat{Z}_\uparrow(\delta \mathbf{k}_n) | \Psi \rangle$ is again given by

the product of the parity eigenvalues at the TRIMs, as expected. This fact requires that the gap at the TRIMs does not close during the adiabatic switching-on of the terms that do not conserve S^z .

[1] C. L. Kane and E. J. Mele, Phys. Rev. Lett. **95**, 226801 (2005), URL <https://link.aps.org/doi/10.1103/PhysRevLett.95.226801>.

[2] B. A. Bernevig, T. L. Hughes, and S.-C. Zhang, Science **314**, 1757 (2006), URL <https://www.science.org/doi/abs/10.1126/science.1133734>.

- [3] M. König, S. Wiedmann, C. Brüne, A. Roth, H. Buhmann, L. W. Molenkamp, X.-L. Qi, and S.-C. Zhang, *Science* **318**, 766 (2007), URL <https://www.science.org/doi/abs/10.1126/science.1148047>.
- [4] M. Z. Hasan and C. L. Kane, *Rev. Mod. Phys.* **82**, 3045 (2010), URL <https://link.aps.org/doi/10.1103/RevModPhys.82.3045>.
- [5] L. Fu, C. L. Kane, and E. J. Mele, *Phys. Rev. Lett.* **98**, 106803 (2007), URL <https://link.aps.org/doi/10.1103/PhysRevLett.98.106803>.
- [6] J. E. Moore and L. Balents, *Phys. Rev. B* **75**, 121306 (2007), URL <https://link.aps.org/doi/10.1103/PhysRevB.75.121306>.
- [7] R. Roy, *Phys. Rev. B* **79**, 195322 (2009), URL <https://link.aps.org/doi/10.1103/PhysRevB.79.195322>.
- [8] C.-K. Chiu, J. C. Y. Teo, A. P. Schnyder, and S. Ryu, *Rev. Mod. Phys.* **88**, 035005 (2016), URL <https://link.aps.org/doi/10.1103/RevModPhys.88.035005>.
- [9] D. J. Thouless, M. Kohmoto, M. P. Nightingale, and M. den Nijs, *Phys. Rev. Lett.* **49**, 405 (1982), URL <https://link.aps.org/doi/10.1103/PhysRevLett.49.405>.
- [10] F. D. M. Haldane, *Phys. Rev. Lett.* **61**, 2015 (1988), URL <https://link.aps.org/doi/10.1103/PhysRevLett.61.2015>.
- [11] L. Fu and C. L. Kane, *Phys. Rev. B* **74**, 195312 (2006), URL <https://link.aps.org/doi/10.1103/PhysRevB.74.195312>.
- [12] L. Fu and C. L. Kane, *Phys. Rev. B* **76**, 045302 (2007), URL <https://link.aps.org/doi/10.1103/PhysRevB.76.045302>.
- [13] L. Fidkowski and A. Kitaev, *Phys. Rev. B* **81**, 134509 (2010), URL <https://link.aps.org/doi/10.1103/PhysRevB.81.134509>.
- [14] Q. Niu, D. J. Thouless, and Y.-S. Wu, *Phys. Rev. B* **31**, 3372 (1985), URL <https://link.aps.org/doi/10.1103/PhysRevB.31.3372>.
- [15] K. Kudo, H. Watanabe, T. Kariyado, and Y. Hatsugai, *Phys. Rev. Lett.* **122**, 146601 (2019), URL <https://link.aps.org/doi/10.1103/PhysRevLett.122.146601>.
- [16] G. E. Volovik, *Zh. Eksp. Teor. Fiz.* **94**, 123 (1988), URL <http://jetp.ras.ru/cgi-bin/e/index/e/67/9/p1804?a=list>.
- [17] G. E. Volovik, *The Universe in a Helium Droplet* (Oxford University Press, 2009).
- [18] V. Gurarie, *Phys. Rev. B* **83**, 085426 (2011), URL <https://link.aps.org/doi/10.1103/PhysRevB.83.085426>.
- [19] A. Blason and M. Fabrizio, *Phys. Rev. B* **108**, 125115 (2023), URL <https://link.aps.org/doi/10.1103/PhysRevB.108.125115>.
- [20] N. Wagner, L. Crippa, A. Amaricci, P. Hansmann, M. Klett, E. J. König, T. Schäfer, D. Di Sante, J. Cano, A. J. Millis, et al., *Nature Communications* **14**, 7531 (2023), URL <https://doi.org/10.1038/s41467-023-42773-7>.
- [21] Z. Wang and S.-C. Zhang, *Phys. Rev. X* **2**, 031008 (2012), URL <https://link.aps.org/doi/10.1103/PhysRevX.2.031008>.
- [22] A. Amaricci, J. C. Budich, M. Capone, B. Trauzettel, and G. Sangiovanni, *Phys. Rev. B* **93**, 235112 (2016), URL <https://link.aps.org/doi/10.1103/PhysRevB.93.235112>.
- [23] A. Amaricci, L. Privitera, F. Petocchi, M. Capone, G. Sangiovanni, and B. Trauzettel, *Phys. Rev. B* **95**, 205120 (2017), URL <https://link.aps.org/doi/10.1103/PhysRevB.95.205120>.
- [24] B. Irsigler, J.-H. Zheng, and W. Hofstetter, *Phys. Rev. Lett.* **122**, 010406 (2019), URL <https://link.aps.org/doi/10.1103/PhysRevLett.122.010406>.
- [25] R. Resta and S. Sorella, *Phys. Rev. Lett.* **82**, 370 (1999), URL <https://link.aps.org/doi/10.1103/PhysRevLett.82.370>.
- [26] I. Gilardoni, F. Becca, A. Marrazzo, and A. Parola, *Phys. Rev. B* **106**, L161106 (2022), URL <https://link.aps.org/doi/10.1103/PhysRevB.106.L161106>.
- [27] S. Barbarino, G. Sangiovanni, and J. C. Budich, *Phys. Rev. B* **99**, 075158 (2019), URL <https://link.aps.org/doi/10.1103/PhysRevB.99.075158>.
- [28] R. Favata, D. Piccioni, A. Parola, and F. Becca, *Phys. Rev. B* **111**, 155105 (2025), URL <https://link.aps.org/doi/10.1103/PhysRevB.111.155105>.
- [29] Z. Wang, X.-L. Qi, and S.-C. Zhang, *New Journal of Physics* **12**, 065007 (2010), URL <https://dx.doi.org/10.1088/1367-2630/12/6/065007>.
- [30] C.-X. Liu, X.-L. Qi, H. Zhang, X. Dai, Z. Fang, and S.-C. Zhang, *Phys. Rev. B* **82**, 045122 (2010), URL <https://link.aps.org/doi/10.1103/PhysRevB.82.045122>.